J Mol Model (2013) 19:2625–2633
DOI 10.1007/s00894-013-1797-9

ORIGINAL PAPER

The substitution reaction of (CNC)Fe_2N_2 with CO

Hongyan Liu · Shuangshuang Liu · Xiang Zhang

Received: 20 November 2012 / Accepted: 5 February 2013 / Published online: 17 March 2013

Abstract The substitution mechanism of two N_2 ligands in (CNC)Fe_2N_2 replaced by CO was studied theoretically at the B3LYP/LACVP* level. Both S_N1 and S_N2 mechanisms were considered. The calculated results for the gas phase suggested that: 1) in S_N1 mechanism, N_2 elimination, which involves S_0-T_1 PESs crossing, is the rate control step for both substitution stages. The barrier heights are 9.7 kcal mol^{-1} and 13.05 kcal mol^{-1}, respectively. 2) In S_N2 mechanism, the calculated barrier heights on LS PES are respectively 13.7 and 19.83 kcal mol^{-1} for the two substitution steps, but S_0-T_1 PESs crossing lowers the two barriers to 10.7 and 15.7 kcal mol^{-1}, respectively. 3) Inclusion of solvation effect of THF by PCM model, the relative energies of all the key species (including minima, transition states and S_0-T_1 crossing points) do not have great difference from their gas phase relative energies. Considering that for each substitution step, S_N1 barrier heights is slightly smaller than S_N2 barrier, S_N1 mechanism seems to be slightly preferable to S_N2 mechanism.

Keywords Barrier heights · (CNC)Fe_2N_2 · CO · N_2 ligands · S_N2 mechanism · S_0-T_1 PESs crossing

Introduction

Transition metal dinitrogen complexes are an active research area since they are considered to be important intermediates in N_2 fixation and activation by artificial systems. It is generally accepted that the activation comes from filling metal d electrons into N_2 π^* orbital. Thus low oxidation state of center metal atom and strong σ-donating ligand are propitious to the activation of N_2. N_2 activation and function by low-valent group 4, 5 and 6 metals have been reported [1–4]. In recent years, low-valent iron dinitrogen complexes have attracted much more attention [5–9]. In 2010, Tylar et al. discussed the recent advances in iron-dinitrogen coordination complexes and their reactivity [10].

Chirik and coworkers [11], and Danopoulos and coworkers [12] reported two types of activated bis-dinitrogen Fe (0) complexes, in which two end-on dinitrogen ligands were supported by the same iron(0) center. In the former, the ligand is ^{iPr}PDI((2,6-CHMe$_2$)$_2$C$_6$H$_3$N=CMe)$_2$C$_5$H$_3$N), while in the later the ligand is CNC ligand(CNC=2,6-bis (aryl-imidazol-2-ylidene)pyridine, aryl=2,6-Pr$^i_2$C$_6$H$_3$). Although the Fe atom in both complexes is in d^8 configuration [8], experimental results claimed a high-spin (HS, triplet) ground state for the former complex but a low-spin (LS, singlet) ground state for the later complex.

In this paper, we present our theoretical investigation to the reaction mechanism of (CNC)Fe_2N_2 with CO, by which two weak electron donor N_2 ligands are replaced by stronger electron donor CO ligands stage by stage, as found in Danopoulos experimental findings [12].

Because CO is a stronger electron donor than N_2, both the replacing steps should be thermodynamically favorable. However, the mechanism and dynamic information of these replacing processes are still kept unknown. Generally, two mechanisms, S_N1 and S_N2, are possible, as shown in Fig. 1. For the simplicity of discussion, we use (CNC)Fe(L_1)_(L_2), where L_1 is the basal ligand while L_2 is the apical ligand, to denote the five coordinates Fe(0) complexes in the following sections. Taking the first replacement reaction for example: 1) if the replacement happens via S_N1 mechanism, (CNC)Fe(N_2)_N_2 first eliminates the axial N_2 to afford a (CNC)Fe(N_2) intermediate, then one CO molecule adds to Fe center to form (CNC)Fe(N_2)_(CO). Normally, the elimination step should need higher activation energy and is the

H. Liu
College of Chemistry and Chemical Engineering, Shanxi Datong University, Datong 037009 Shanxi Province, China

S. Liu · X. Zhang (✉)
School of Chemistry & Material Sciences, Shanxi Normal Uniovsersity, Linfen 041004, China
e-mail: xiangzh2000@hotmail.com

H. Liu
Department of Chemical and Petroleum Engineering, University of Wyoming, Laramie, WY 82071, USA

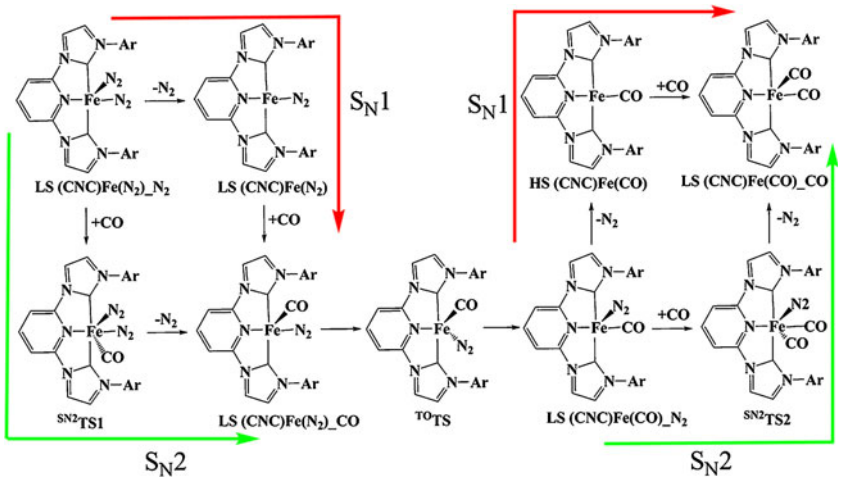

Fig. 1 S_N2 and S_N1 mechanism for substituting two N_2 ligands of (CNC)Fe(N_2)_N_2 by two CO molecules

rate control step. 2) If the replacement happens via S_N2 mechanism, a transition state will be formed when one CO molecule attacks the Fe center from the opposite direction of apical N_2 ligand, through which the breaking of Fe-N bond and the forming of C-Fe bond occur simultaneously. The second N_2 replacement by CO step may have similar mechanisms. In this paper, we present a detailed theoretical investigation on the two mechanisms, and our results suggest that S_0-T_1 crossings are important for both S_N1 and S_N2 mechanisms, and lowers the barriers, which is more favorable for both the substitution steps.

Computational methods

We employed hybrid B3LYP [13–15], which utilizes the three-parameter exchange functionals of Backe in conjunction with the Lee-Yang-Parr correlation functional in our calculations. LACVP* basis set [6-31G(d) for H, C, N and O atoms and LANL2DZ basis set and ECP (ten core electrons) for Fe] [16, 17], which has been extensively used to study the compounds containing Fe [18–20]. For stable points, including minima and transition states, all the geometries were optimized without any constraint, and their vibration frequencies were calculated at the same level of optimization. The intrinsic reaction coordinate (IRC) method was used to track minimum energy paths from transition state structures to the corresponding minimum. Searching for S_0-T_1 crossing points (where a geometry has the same electronic energy on both LS and LH potential energy surfaces) in the S_N1 mechanisms, flexible scans along a serials fixed apical Fe-N distances were carried out for (CNC)Fe(N_2)-N_2 and (CNC)Fe(CO)-N_2 on both LS and HS PESs, followed by point wise single energy calculations on the opposite PESs. The crossing points in the S_N2 mechanisms were obtained by calculating the HS electronic energies at the geometries along the LS MEPs. When considering solvation effect of THF, SCRF single point energies were calculated with default parameters using PCM model [21–23].

Al calculations were were performed using Gaussian 03 program [24] except for SCRF calculations for which Gaussian 09 was used [25].

Results and discussion

Figure 2 depicts all the optimized geometries of the stable species, including minima and transition states, with the key geometric parameters. For comparation, the calculated and experimental key bond lengths of LS (CNC)Fe(N_2)_N_2 and LS (CNC)Fe(CO)_CO are given in Tables 1 and 2. It can be seen that, most calculated bond lengths are in good agreement with the experimental values in ref. [12]. The great differences come from Fe-N3 (0.032 Å), Fe-C1 (0.039 Å) of LS (CNC)Fe(N_2)_N_2, and Fe-C2 (0.028 Å) of LS (CNC)Fe(CO)_CO. Considering that the calculated values correspond to isolated molecules while the measured bond lengths are for single crystals, these differences are not significant and the theoretical method used in this study is reliable.

In the following sections, we will first present the reaction profiles of the S_N1 mechanism, and then discuss the S_N2 mechanism with the relative energies for gas phase. Solvation effect of THF to the relative energies will be considered in the last part. It should be noted that in the following discussion, energies about S_0-T_1 PES crossing are the relative electronic energy values without ZPE correction while the other energies values are the relative electronic energy values with ZPE correction.

S_N1 mechanism

Figure 3a depicts the reaction profiles of S_N1 mechanism for the first substitution step, and Fig. 3b depicts the S_0-T_1 crossing profiles of $^{OPT}S_0$ with $^{SP}T_1$ and $^{SP}S_0$ with $^{OPT}T_1$ in the process of first N_2 elimination, with the relative energies of the stable structures involved. In another paper [26], we have discussed the N_2 elimination mechanism from LS (CNC)Fe(N_2)_N_2, and

concluded that an S_0-T_1 PESs crossing mechanism, which lowers the barrier to 9.7 kcal mol^{-1} and affords four-member coordinated intermediate HS (CNC)Fe(N_2), is more favorable. From Fig. 3a, we can see that the addition of CO onto LS (CNC)Fe(N_2) and HS (CNC)Fe(N_2) are greatly exothermal, by 43.5 and 27.59 kcal mol^{-1} respectively, to produce LS (CNC)Fe(N_2)_CO. Since CO is a stronger electron donor than N_2, we may expect that the barrier of CO addition to HS (CNC)Fe(N_2) should be smaller than that of N_2 addition. Therefore, the S_N1 barrier for the first N_2 to CO replacement reaction can be taken at the S_0-T_1 crossing point **CRP1**, 9.7 kcal mol^{-1}. The details of the addition step will not be discussed.

Figure 4a depicts the reaction profiles of S_N1 mechanism for the second substitution step, and Fig. 4b depicts the S_0-T_1 crossing profiles of $^{OPT}S_0$ with $^{SP}T_1$ and $^{SP}S_0$ with $^{OPT}T_1$ in the process of second N_2 elimination. As the products in the first substitution step, (CNC)Fe(N_2)_CO is in its LS ground state. It can easily convert to LS (CNC)Fe(CO)_N_2 via a small barrier of 3.53 kcal mol^{-1}. The N_2 elimination intermediate of (CNC)Fe(CO)_N_2, four-member-coordinated Fe(0) complex (CNC)Fe(CO), also prefers HS ground state. Relative to the total energy of LS (CNC)Fe(CO)_N_2, the relative energies of LS (CNC)Fe(CO) + N_2 and HS (CNC)Fe(CO) + N_2 are respectively 18.03 and 13.05 kcal mol^{-1}. Therefore, in the course of N_2 elimination from (CNC)Fe(CO)_N_2, S_0-T_1 spin conversion will happen and similar S_0-T_1 PES crossing is possible. From Fig. 4a and b, we can see that the lower energy channel of N_2 elimination from (CNC)Fe(CO)_N_2 also involves an S_0-T_1 crossing mechanism. This nonadiabatic mechanism exists in most reactions [27–31]. However,

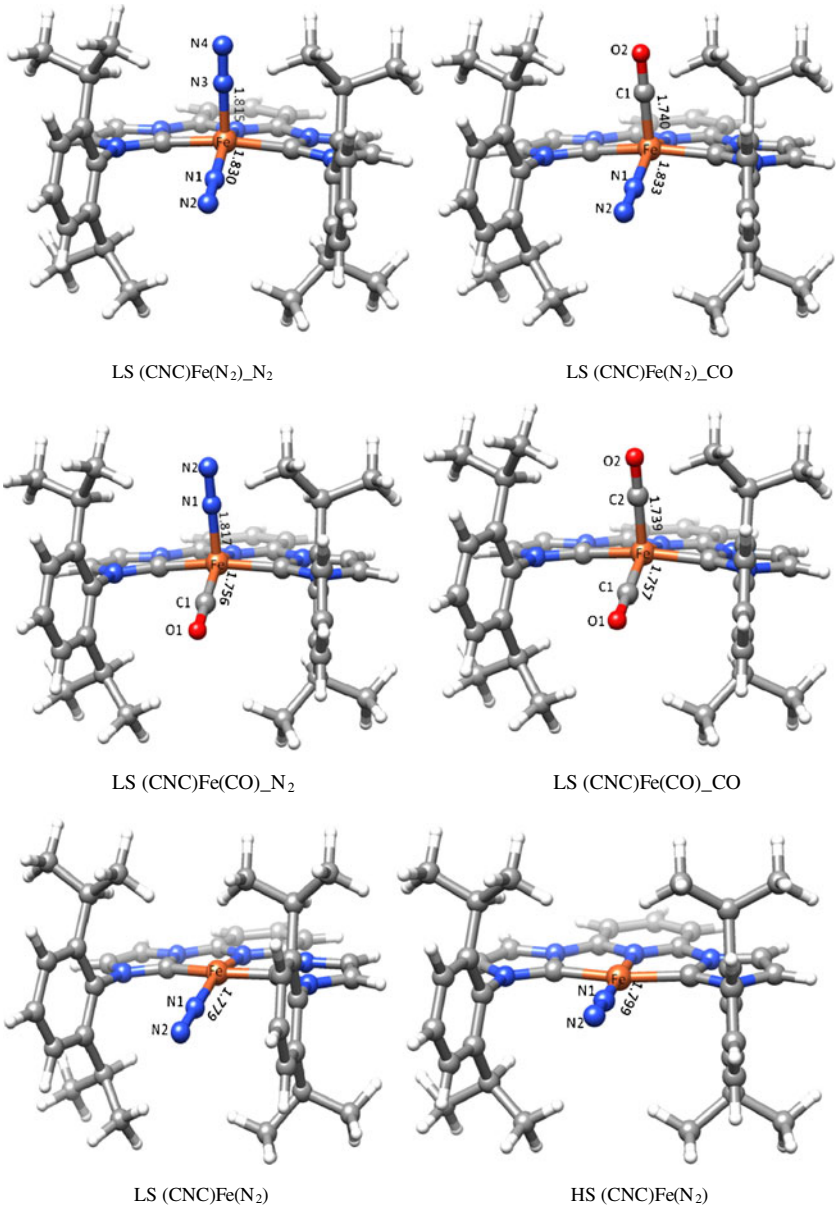

Fig. 2 Optimized geometries of the stable species, including minima and transition states of the two substitution steps via S_N2 mechanism

Fig. 2 (continued)

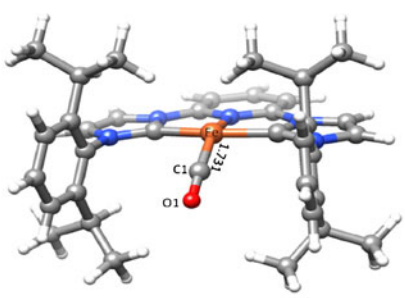

LS (CNC)Fe(N_2)

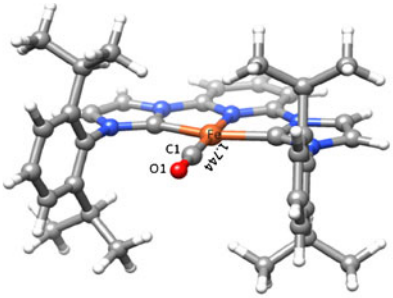

HS (CNC)Fe(N_2)

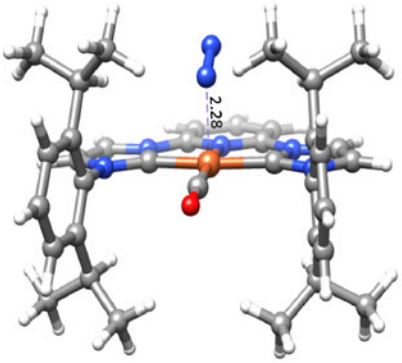

^{S0}TS

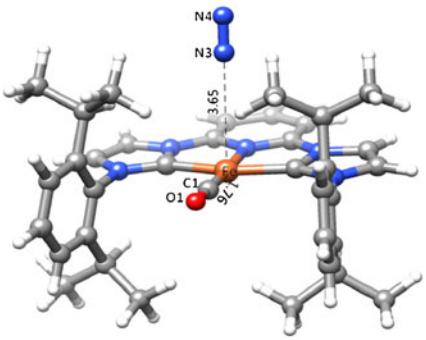

HS (CNC)Fe(CO)---N_2 complex

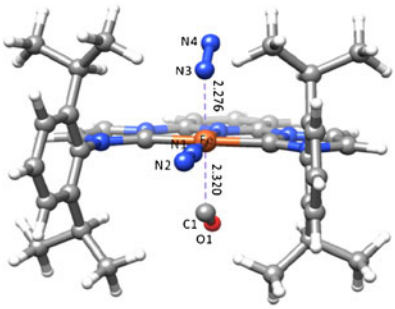

^{SN2}TS1

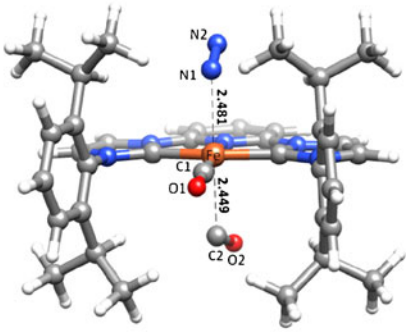

^{SN2}TS2

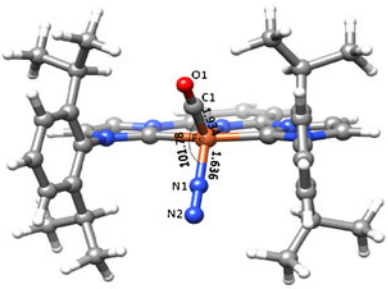

^{TO}TS

different from the S_0-T_1 crossing mechanism in the first N_2 elimination step, the S_0-T_1 crossing point of the second N_2 elimination (**CRP2**) is not the highest energy point along the N_2 elimination path since it is lower than HS (CNC)Fe(CO) + N_2 by 0.65 kcal mol^{-1}. Checking the $^{OPT}T_1$ profile, it decreases monotonously with the increase of Fe-N1 distance in the scan region but at the long end of Fe-N1 bond, the relative energies of $^{OPT}T_1$ points are lower than the relative energy of

Table 1 Claculated and experimental bond lengths of LS (CNC)Fe(N_2)_N_2 and (CNC)Fe_2CO (in Å)

	Calculated	Ref. [12]		Calculated	Ref. [12]
Fe-N1	1.831	1.820	Fe1-C1	1.757	1.746
Fe-N3	1.815	1.847	Fe-C2	1.739	1.767
N1-N2	1.124	1.113	C1-O1	1.166	1.165
N3-N4	1.125	1.115	C2-O2	1.167	1.161
Fe-C1	1.951	1.912	Fe-C3	1.933	1.918
Fe-C2	1.951	1.915	Fe-C4	1.933	1.910
Fe-N5	1.899	1.890	Fe-N1	1.917	1.843

HS (CNC)Fe(CO) + N_2, 13.05 kcal mol^{-1}. This result implies that an HS (CNC)Fe(CO)—N_2 complex may exist. We found this HS (CNC)Fe(CO)—N_2 complex, in which the Fe-N1 distance is 3.65 Å. It seems that the stability of the HS (CNC)Fe(CO)—N_2 complex is not too poor since its decomposition barrier (to HS (CNC)Fe(CO) + N_2) is about 6.43 kcal mol^{-1} and its barrier for forming LS (CNC)Fe(CO)_N_2 is 5.78 kcal mol^{-1} (relative to CRP2). If these well depth values are reliable, it is possible that the HS (CNC)Fe(CO)—N_2 complex can be detected by experimental methods at low temperature.

Paying attention to $^{OPT}S_0$ profile, one can see that, at the long-end of Fe-N1 bond, the relative energies are even higher than the relative energy of LS (CNC)Fe(CO) + N_2, 18.03 kcal mol^{-1}. This implies the existence of a transition state on the S_0 PES, ^{S0}TS. We had trouble in accurately locating the structure of ^{S0}TS, probably due to the very loose structure and very flat PES in the region of ^{S0}TS. An approximate ^{S0}TS structure with a long Fe-N1 bond of about 3.35 Å is given in Fig. 2. ^{S0}TS is about 25.74 kcal mol^{-1} higher than LS (CNC)Fe(CO)_N_2. Such a high barrier means that, the reaction rate of N_2 elimination through ^{S0}TS is negligible.

Table 2 Relative energies of the stable species involved in S_N2 mechanism

	Relative energy (kcal mol^{-1})	
	LS E_e + ZPE/E_e	HS (E_e) E_e
(CNC)Fe(N_2)_N_2	0.00/*0.00*	*19.15* (19.15)[b]
^{SN2}TS1	13.70/*14.33*	*7.32* (-7.01)
(CNC)Fe(N_2)_CO	−26.60/*−27.47*	*1.59* (29.06)
(CNC)Fe(CO)_N_2	−24.82/*−25.85*	*−1.90*(23.95)[c]
^{SN2}TS2	−4.99/*−4.25*	*−14.13* (−9.88)
(CNC)Fe(CO)_CO	−51.63/*−53.17*	*−57.42*(−4.25)

*Values in italic are without ZPE correction

**values in parentheses are relative electronic energies of HS species corresponding to LS species

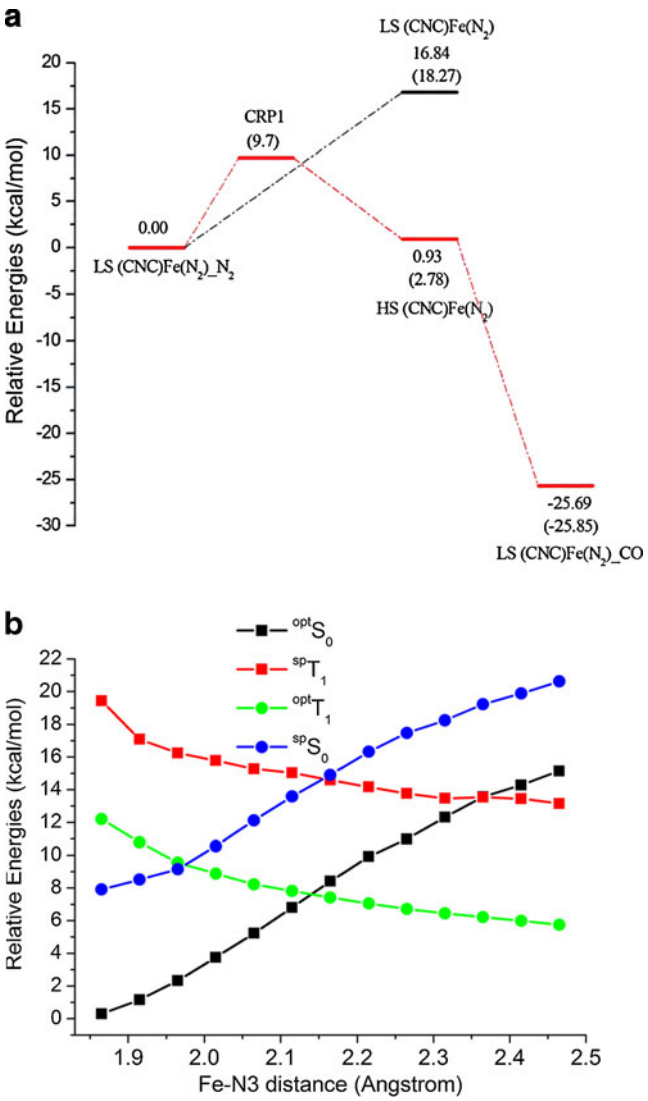

Fig. 3 **a** S_N1 mechanism for N_2 of LS-(CNC)Fe(N_2)_N_2 replaced by CO. Relative energies are calculated from E_e + ZPE. Values in parentheses are relative energies without ZPE correction. **b** S_0-T_1 crossing position in the first N_2 elimination process. $^{opt}S_0$, point wise-optimized S_0 state profile; $^{sp}T_1$, single-point energy profile based on $^{opt}S_0$ geometries; $^{opt}T_1$, point wise-optimized T_1 state profile; $^{sp}S_0$, single-point energy profile based on $^{opt}T_1$ geometries

CO addition onto the HS (CNC)Fe(CO) will finally result in singlet five-member coordinated Fe(0) complexes and may involve HS (CNC)Fe(CO)—CO complex and a T_1-S_0 state crossing point. However, we can assert without doubt that HS (CNC)Fe(CO)—CO complex and the T_1-S_0 state crossing point are both located lower than HS (CNC)Fe (CO) + CO, based on the fact that CO is a stronger electron donor and the addition is exothermal 39.86 kcal mol^{-1}. Therefore, the addition of CO onto HS (CNC)Fe(CO) to finally afford LS (CNC)Fe(CO)_CO is indeed a barrier free process. The S_N1 mechanism activation barrier of the N_2 of LS (CNC)Fe(CO)_N_2 replaced by CO should equal to the N_2 elimination barrier through S_0-T_1 state crossing mechanism, 13.05 kcal mol^{-1}.

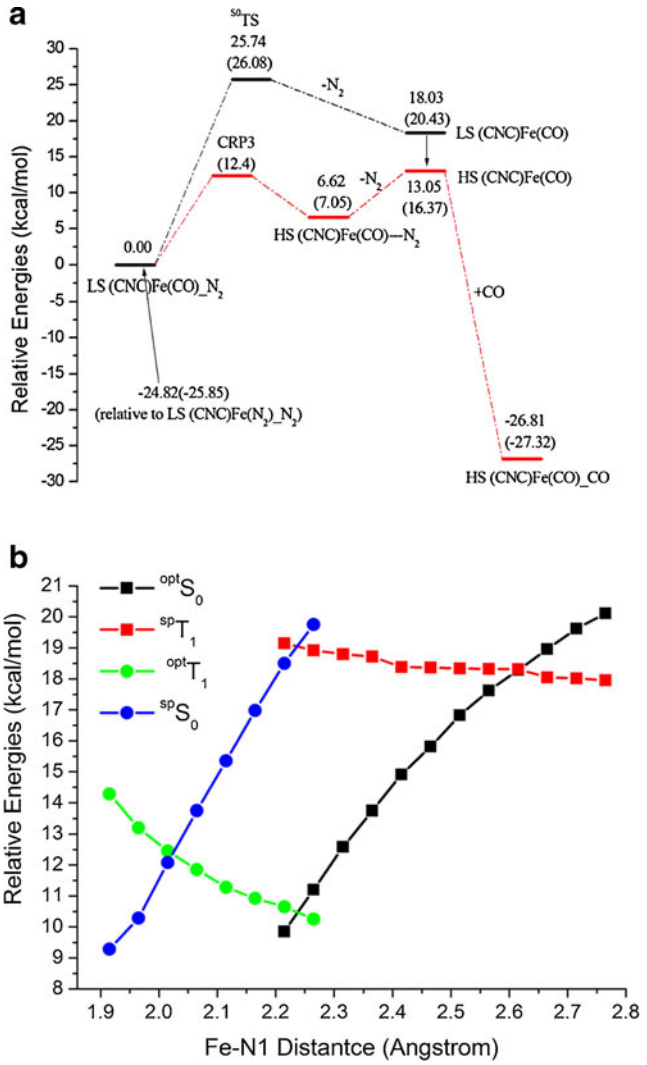

Fig. 4 **a** S_N1 mechanism for N_2 of LS-(CNC)Fe(CO)_N_2 replaced by CO. Relative energies are calculated from E_e + ZPE. Values in parentheses are relative energies without ZPE correction. **b** S_0-T_1 crossing position in the second N_2 elimination process. $^{opt}S_0$, point wise-optimized S_0 state profile; $^{sp}T_1$, single-point energy profile based on $^{opt}S_0$ geometries; $^{opt}T_1$, point wise-optimized T_1 state profile; $^{sp}S_0$, single-point energy profile based on $^{opt}T_1$ geometries

S_N2 mechanism

Figure 5a to5c summarizes the S_N2 mechanism for substituting two N_2 ligands of (CNC)Fe(N_2)_N_2 by two CO molecules based on B3LYP theoretical calculations.

As shown in Fig. 5a, on the S_0 PES, replacing the two N_2 ligands by two CO molecules via S_N2 mechanism consists of three steps: 1) S_N2 replacement of apical N_2 of (CNC)Fe (N_2)_N_2 by first CO molecule; 2) structural turnover of intermediate product which changes the situation of apical CO and basal N_2 ligands; 3) S_N2 replacement of apical N_2 of (CNC)Fe(CO)_N_2 by second CO molecule, to afford final (CNC)Fe(CO)_CO. ^{SN2}TS1, ^{TO}TS2 and ^{SN2}TS2 are used to denote the three transition states in first S_N2 substitution step, conversion between (CNC)Fe(N_2)_CO and (CNC)Fe (CO)_N_2, and in second S_N2 substitution step.

In the first S_N2 substitution step, C1-O1 molecule replaces the axial N3-N4 of (CNC)Fe(N_2)_N_2, by attacking Fe center from the opposite direction of N3-N4. In the transition state of ^{SN2}TS1, the Fe-N3 bond has been elongated to 2.276 Å and the Fe-C1 bond is 2.320 Å. The reaction mode has an imaginary frequency of *i*481 cm^{-1}. The barrier height of ^{SN2}TS1 is 13.70 kcal mol^{-1}. The product (CNC)Fe(N_2)_CO is a distorted square pyramid, which has basal N1-N2 ligand and apical C1-O1 ligand. This step is exothermal by 26.60 kcal mol^{-1}.

Required by spatial effect, to substitute the second N_2 ligand by CO molecule needs a structural turnover from (CNC)Fe(N_2)_CO to (CNC)Fe(CO)_N_2, so that the second N_2 ligand is positioned as the apical ligand. This turnover happens through a transition state, ^{TO}TS. The forward and reverse barrier heights are only 3.47 and 1.69 kcal mol^{-1}. Such small barrier heights for forward and reverse reactions suggest a nearly free conversion between (CNC)Fe(N_2)_CO and (CNC)Fe(CO)_N_2 at room temperature. A similar transition state can also be found for configuration turnover of (CNC)Fe (N_2)_N_2, and configuration turnover of (CNC)Fe(CO)_CO, with very small barrier height. For example, a conversion transition state between (CNC)Fe(C1O1)_C2O2 and (CNC) Fe(C2O2)_C1O1 gives a barrier height of 1.53 kcal mol^{-1}.

In the second S_N2 substitution step, the second CO molecule attacks Fe center from the opposite direction of apical N1-N2 ligand of (CNC)Fe(CO)_N_2, forms the transitions state ^{SN2}TS2. The Fe-N3 bond is elongated to 2.481 Å and Fe-C2 bond is 2.449 Å. The reaction mode of ^{SN2}TS2 has an imaginary frequency of *i*423 cm^{-1}. The barrier height is 19.83 kcal mol^{-1}. The final product (CNC)Fe(CO)_CO is also a distorted square pyramid, with one basal and one apical CO ligand. The second S_N2 substitution step is exothermal 25.81 kcal mol^{-1}.

From above results, we can see that, on the LS PES, the barrier heights of the two S_N2 substitution steps are higher than those of S_N1 mechanism which involves S_0-

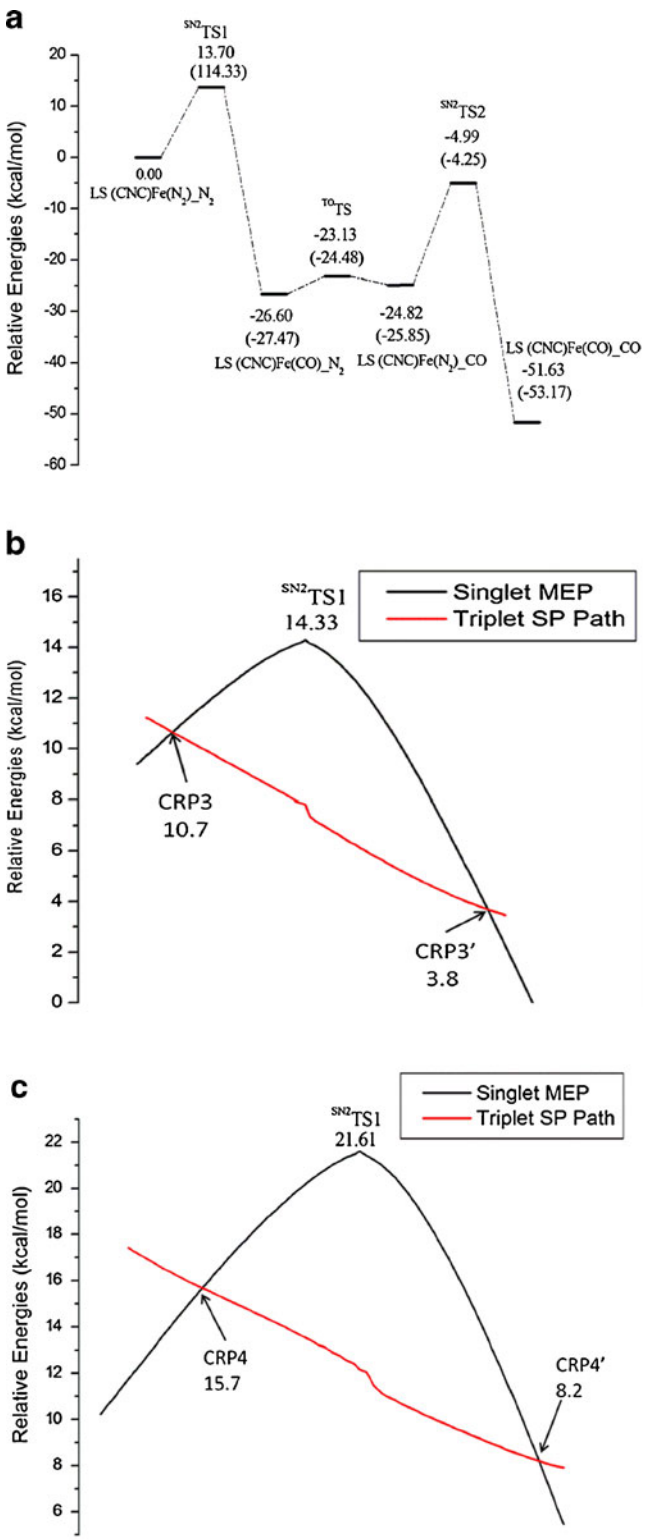

Fig. 5 **a** Energy profiles of S_N2 mechanism of N_2 substitution reaction of (CNC)Fe(N_2)_N_2 by CO on the S_0 PES; 5b) S_0-T_1 crossing in the first S_N2 step; 5c) S_0-T_1 crossing in the second S_N2 step *Energies are calculated from electronic energies only; **In 5b, energy values are relative to (CNC)Fe(N_2)_N_2 plus CO, while in 5c, energy values are relative to (CNC)Fe(CO)_N_2 plus CO

T_1 crossing. However, S_0-T_1 PES crossing is also possible in the S_N2 mechanism. At the B3LYP/LACVP* level, we calculated the T_1 state electronic energies at the geometries of LS (CNC)Fe(N_2)_N_2, ^{SN2}TS1, LS (CNC)Fe(N_2)_CO, LS (CNC)Fe(CO)_N_2, ^{SN2}TS2 and LS (CNC)Fe(CO)_CO. The results are summarized in Table 3. It can be seen that, for all the minima, their T_1 state energies are all higher than their S_0 state energies, but for the ^{SN2}TS1 and ^{SN2}TS2, the T_1 state electronic energies are respectively by 7.01 and 9.88 kcal mol^{-1} smaller than their S_0 state electronic energies. Therefore, it is quite possible that the N_2 elimination via S_N2 mechanism may happen through an S_0-T_1 PES crossing path.

To accurately determine the S_0-T_1 crossing region is a very difficult task and what we can do is to estimate the position of crossing point and its relative energy by pointwise energy calculations for both S_0 and T_1 states at the geometries along the minimum energy path of LS S_N2 mechanism. In Fig. 5b and c, the S_0-T_1 crossing profiles of the first and second substitutions calculated at the B3LYP/LACVP* level are depicted, respectively.

Table 3 Calculated relative energies of the stable species in gas phase and in THF solution (relative electronic energies, in kcal mol^{-1})

		Gas phase	THF solution
LS (CNC)Fe(N_2)_N_2		0.00	0.00
LS (CNC)Fe(N_2)_CO		−27.47	−26.41
LS (CNC)Fe(CO)_N_2		−25.85	−25.22
LS (CNC)Fe(CO)_CO		−53.17	−52.47
LS_CNC_Fe(N_2)		18.27	18.52
HS CNC_Fe(N_2)		2.77	4.09
LS_CNC_Fe(CO)		−5.43	−4.51
HS CNC_Fe(CO)		−9.49	−10.88
^{SN1}TS		−3.39	−2.17
HS CNC_Fe(CO)—N_2		−18.14	−17.26
^{SN2}TS1		14.33	14.50
^{SN2}TS2		−4.25	−4.09
^{TO}TS		−24.48	−23.25
CRP1	LS	8.53	8.73
	HS	8.53	10.97
CRP2	LS	−13.50	−13.64
	HS	−13.50	−11.55
CRP3	LS	10.66	11.78
	HS	10.66	12.96
CRP4	LS	−10.42	−8.89
	HS	−10.42	−8.21

*Geometries of crossing points were approximately chosen (the optimized point which is closest to the crossing point in flexible scan or IRC calculations)

From Fig. 5b, we can see that, in the region of transition state ^{SN2}TS1, T_1 state is lower than S_0 state, and from the reactant side to product side, the T_1 SP path monotonously decreases with the reaction coordinate increasing. T_1 SP path crosses with S_0 MEP at both the reactant side and product side, and the two crossing points (**CRP3** and **CRP3'**) are located lower than ^{SN2}TS1 by 3.6 and 10.5 kcal mol^{-1}. This result suggests that the first S_N2 reaction may undergo an S_0-T_1-S_0 path which involves two S_0-T_1 crossing points, and the highest barrier is at the first crossing point, which has relative energy about 10.7 kcal mol^{-1} (relative to (CNC)Fe(N_2)_N_2 plus CO).

From Fig. 5c, we can see that the second S_N2 substitution reaction may proceed via similar S_0-T_1-S_0 path, along which the reactant side crossing point(**CRP4**) and the product side crossing point (**CRP4'**) are located 5.9 and 13.4 kcal mol^{-1} lower than ^{SN2}TS2, respectively. Therefore, relative to (CNC)Fe(CO)_N_2 plus CO, the barrier height for the second substitution along the S_0-T_1-S_0 crossing path should be about 15.7 kcal mol^{-1} (relative to (CNC)Fe(CO)_N_2 plus CO).

From the above discussions, we can see that, for both substitution steps, the barrier heights of S_N2 mechanism involving S_0-T_1-S_0 PES crossing are slightly greater than corresponding barriers of S_N1 mechanism involving S_0-T_1 crossing. Therefore, S_N1 and S_N2 mechanisms are competitive in both substitution steps. Considering that, all the barrier heights along the S_0-T_1 crossing PESs are not higher than 15 kcal mol^{-1}, two N_2 ligands replacement by two CO molecules should be kinetically quite fast at room temperature. This conclusion is consistent with the experimental result [12].

Solvation effect of THF to the relative energies

When considering the solvation effect of THF on the relative energies, we provided the relative electronic energies (without ZPE correct) for all the stable points and crucial crossing points in Table 3. From Table 3, we can see that all of the relative energies with solvation effect are close to these values in gas phase. So the main conclusion obtained for gas phase will not be changed when solvation effect of THF is included.

Conclusions

In this paper, we studied the mechanism of two N_2 ligands of (CNC)Fe(N_2)_N_2 substituted by CO molecules. For S_N1 mechanism, N_2 elimination from (CNC)Fe(N_2)_N_2 and (CNC)Fe(CO)_N_2 is the rate control step, which involves S_0-T_1 PES crossing and results in triplet intermediates (CNC)Fe(N_2) and (CNC)Fe(CO). S_0-T_1 PES crossing lowers the elimination barriers of the first and second steps to 9.7 and 13.05 kcal mol^{-1}, respectively. On the LS PES, the barrier heights of the first and second S_N2 steps were calculated to be 13.7 kcal mol^{-1} and 19.83 kcal mol^{-1}, respectively. S_0-T_1 PES crossing is also possible for S_N2 reaction, and lowers the S_N2 barrier heights of the two substitution steps to 10.7 and 15.7 kcal mol^{-1}, respectively. Including solvation effects of THF do not significantly change the relative energies of all the minima, transition states and crossing points. Therefore, S_N1 mechanism which involves S_0-T_1 PES crossing is slightly preferred to S_N2 mechanism for two N_2 ligands of (CNC)Fe(N_2)_N_2 substituted by two CO molecular.

Acknowledgments The Project is supported by the Scientific Research Foundation for the Returned Overseas Chinese Scholars, Shanxi Province, P. R. China. Project No. 2008–75.

References

1. Morello L, Yu P, Carmichael CD, Patrick BO, Fryzuk MD (2005) Formation of phosphorus-nitrogen bonds by reduction of a titanium phosphine complex under molecular nitrogen. J Am Chem Soc 127:12796
2. McKay BA, Fryzuk MD (2004) Dinitrogen coordination chemistry: on the biomimetic borderlands. Chem Rev 104:385
3. Schrock RR (2003) Catalytic reduction of dinitrogen under mild conditions Chem Commun 2389–2391
4. Gambarotta S, Scott J (2004) Multimetallic cooperative activation of N_2. Angew Chem Int Ed 43:5298–5308
5. Leigh GJ (1992) Protonation of coordination dinitrogen. Acc Chem Res 25:177–181
6. Hirano M, Akita M, Morikita T, Kubo H, Fukuoka A, Komiya S (1997) Synthesis, structure and reactions of a dinitrogen complex of iron(0), [Fe(N-2)(depe)(2)] (depe equals Et2PCH2CH2PEt2) J Chem Soc Dalton Trans pp 3453–3458
7. Hills A, Hughes DL, Jimenez-Tenorio M, Leigh GJ (1993) Bis [1,2- bis(dimethylphosphino) ethane]dihydrogen hydrido-iron(II) tetraphenylborates as a model for the function of nitrogenases. J Chem Soc Dalton Trans pp 3041–3049
8. Andres A, Bominaar EL, Smith JM, Eckert NA, Holland PL, Munck E (2002) Planar three-coordinate high-spin Fe-II complexes with large orbital angular momentum: Mossbauer, electron paramagnetic resonance, and electronic structure studies. J Am Chem Soc 124:3012–3025
9. Betley TA, Peters JC (2004) A tetrahedrally coordinated L3Fe-N-x platform that accommodates terminal nitride (Fe-IV N) and dinitrogen (Fe-I-N-2-Fe-I) ligands. J Am Chem Soc 126:6252–6254
10. Crossland JL, Tylar DR (2010) Iron-dinitrogen coordination chemistry: dinitrogen activation and reactivity coordination. Chem Rev 254:1883–1894
11. Bart SC, Lobkovsky E, Chirik PJ (2004) Preparation and molecular and electronic structures of iron (0) dinitrogen and silane complexes and their application to catalytic hydrogenation and hydrosilation. J Am Chem Soc 126:13794–13807
12. Danopoulos AA, Wrighta JA, Motherwell WB (2005) Molecular N_2 complexes of iron stabilised by N-heterocyclic 'pincer' dicarbene ligands. Chem Commun pp 784–786

13. Becke AD (1993) Density-functional thermochemistry 3: the role of exact exchange. J Chem Phys 98:5648–5652
14. Lee C, Yang W, Parr RG (1988) Development of the colle-salvetti correlation-energy formula into a functional of the electron-density. Phys Rev B 37:785–789
15. Miehlich B, Savin A, Stoll H, Preuss H (1989) Results obtained with the correlation-energy density functionals of Becke and Lee, Yang and Parr. Chem Phys Lett 157:200–206
16. Dunning TH, P. J. Hay PJ (1976) In: Schaefer HF (ed), Modern theoretical chemistry. Plenum, New York
17. Friesner RA RA, Murphy RB RB, Beachy MD MD, Ringlanda MN MN, Pollard WT, Dunietz BD, Cao YX (1999) Correlated ab initio electronic structure calculations for large molecules. J Phys Chem A 103:1913–1928
18. Li DM, Wang Y, Han KL (2012) Recent density functional theory model calculations of drug metabolism by cytochrome P450. Coordination Chem Rev 256:1137–1150
19. Li DM, Xiaoqin HX, Han KL, Zhan CG (2011) Catalytic mechanism of cytochrome P450 for 5 '-Hydroxylation of nicotine: fundamental reaction pathways and stereoselectivity. J Am Chem Soc 133:7416–7427
20. Li DM, Wang YY, Han KL, Zhan CG (2010) Fundamental reaction pathways for cytochrome P450-catalyzed 5 '-hydroxylation and N-demethylation of nicotine. J Phys Chem B 114:9023–9030
21. Miertus S, Tomasi J (1982) Approximate evaluations of the electrostatic free-energy and internal energy changes in solution processes. Chem Phys 65:239–245
22. Miertus S, Scrocco E, Tomasi J (1981) Electrostatic interaction of a solute with a continuum - a direct utilization of abinitio molecular potentials for the prevision of solvent effects. Chem Phys 55:117–129
23. Cossi M, Barone V, Mennucci B, Tomasi J (1998) Ab initio study of ionic solutions by a polarizable continuum dielectric model. Chem Phys Lett 286:253–260
24. Gaussian 03, Revision C.02: Frisch MJ, Trucks GW, Schlegel HB, Scuseria GE, Robb MA, Cheeseman JR, Montgomery JA Jr, Vreven T, Kudin KN, Burant JC, Millam JM, Iyengar SS, Tomasi J, Barone V, Mennucci B, Cossi M, Scalmani G, Rega N, Petersson GA, Nakatsuji H, Hada M, Ehara M, Toyota K, Fukuda R, Hasegawa J, Ishida M, Nakajima T, Honda Y, Kitao O, Nakai H, Klene M, Li X, Knox JE, Hratchian HP, Cross JB, Bakken V, Adamo C, Jaramillo J, Gomperts R, Stratmann RE, Yazyev O, Austin AJ, Cammi R, Pomelli C, Ochterski JW, Ayala PY, Morokuma K, Voth GA, Salvador P, Dannenberg JJ, Zakrzewski VG, Dapprich S, Daniels AD, Strain MC, Farkas O, Malick DK, Rabuck AD, Raghavachari K, Foresman JB, Ortiz JV, Cui Q, Baboul AG, Clifford S, Cioslowski J, Stefanov BB, Liu G, Liashenko A, Piskorz P, Komaromi I, Martin RL, Fox DJ, Keith T, Al-Laham MA, Peng CY, Nanayakkara, A, Challacombe M, Gill PMW, Johnson B, Chen W, Wong MW, Gonzalez C, Pople JA (2004) Gaussian, Inc., Wallingford, CT
25. Gaussian 09, Revision C.01, Frisch MJ, Trucks GW, Schlegel HB, Scuseria GE, Robb MA, Cheeseman JR, Scalmani G, Barone V, Mennucci B, Petersson GA, Nakatsuji H, Caricato M, Li X, Hratchian HP, Izmaylov AF, Bloino J, Zheng G, Sonnenberg JL, Hada M, Ehara M, Toyota K, Fukuda R, Hasegawa J, Ishida M, Nakajima T, Honda Y, Kitao O, Nakai H, Vreven T, Montgomery JA, Jr, Peralta JE, Ogliaro F, Bearpark M, Heyd JJ, Brothers E, Kudin KN, Staroverov VN, Keith T, Kobayashi R, Normand J, Raghavachari K, Rendell A, Burant JC, Iyengar SS, Tomasi J, Cossi M, Rega N, Millam JM, Klene M, Knox JE, Cross JB, Bakken V, Adamo C, Jaramillo J, Gomperts R, Stratmann RE, Yazyev O, Austin AJ, Cammi R, Pomelli C, Ochterski JW, Martin RL, Morokuma K, Zakrzewski VG, Voth GA, Salvador P, Dannenberg JJ, Dapprich S, Daniels AD, Farkas O, Foresman JB, Ortiz JV, Cioslowski J, Fox DJ (2010), Gaussian, Inc., Wallingford, CT
26. Zhang X (2010) Theoretical study on the electronic structure of (CNC)Fe_2N_2 and its N_2 elimination mechanism. Int J Quantum Chem 110:1880–1889
27. Chu TS, Zhang Y, Han KL (2006) The time-dependent quantum wave packet approach to the electronically nonadiabatic processes in chemical reactions. Int Rev Phys Chem 25:201–235
28. Xie TX, Zhang Y, Zhao MY, Han KL (2003) Calculations of the F + HD reaction on three potential energy surface. Phys Chem Chem Phys 5:2034–2038
29. Chu TS, Han KL (2008) Effect of Coriolis coupling in chemical reaction dynamics. Phys Chem Chem Phys 10:2431–2441
30. Han KL, He GZ (2007) Photochemistry of aryl halides: photodissociation dynamics. J Photochem Photobiol C Photochem Rev 8:55–66
31. Chu TS, Han KL (2005) Nonadiabatic time-dependent wave packet study of D^++H_2 reaction system. J Phys Chem A 109:2050–2056